

Observation of amplification of light by Langmuir waves and its saturation on the electron kinetic timescale

R. K. KIRKWOOD¹, Y. PING¹, S. C. WILKS¹, N. MEEZAN¹,
P. MICHEL¹, E. WILLIAMS¹, D. CLARK¹, L. SUTER¹,
O. LANDEN¹, N. J. FISCH², E. J. VALEO², V. MALKIN²,
D. TURNBULL², S. SUCKEWER², J. WURTELE³,
T. L. WANG⁴, S. F. MARTINS⁴, C. JOSHI⁴, L. YIN⁵,
B. J. ALBRIGHT⁵, H. A. ROSE⁵ and K. J. BOWERS⁵

¹Lawrence Livermore National Laboratory, Livermore, California 94550, USA

²Department of Astrophysical Sciences, Princeton University, Princeton,
New Jersey 08544, USA

³Department of Physics, University of California at Berkeley, Berkeley,
California 94720, USA

⁴Department of Electrical Engineering, University of California at Los Angeles,
Los Angeles, California 90095, USA

⁵Los Alamos National Laboratory, Los Alamos, New Mexico 87545, USA

(Received 19 October 2010; accepted 16 November 2010;
first published online 21 December 2010)

Abstract. Experiments demonstrate the $\sim 77\times$ amplification of 0.5 to 3.5-ps pulses of seed light by interaction with Langmuir waves in a low density ($1.2 \times 10^{19} \text{ cm}^{-3}$) plasma produced by a 1-ns, 230-J, 1054-nm pump beam with $1.2 \times 10^{14} \text{ W/cm}^2$ intensity. The waves are strongly damped ($k\lambda_D = 0.38$, $T_e = 244 \text{ eV}$) and grow over $a \sim 1 \text{ mm}$ length, similar to what is experienced by scattered light when it interacts with crossing beams as it exits an ignition target. The amplification reduces when the seed intensity increases above $\sim 1 \times 10^{11} \text{ W/cm}^2$, indicating that saturation of the plasma waves on the electron kinetic time scale ($< 0.5 \text{ ps}$) limits the scatter to $\sim 1\%$ of the available pump energy. The observations are in agreement with 2D PIC simulations in this case.

1. Introduction

The amplification of light by the seeded stimulated Raman scattering (SRS) is important for the development of laser-driven inertial confinement fusion. Uncontrolled amplification of light leaving the target can limit the coupling efficiency in indirect drive targets [1]; in addition, an appropriate choice of beam and plasma conditions promises to produce higher power and improved focal quality beams via the combined processes of plasma amplification and pulse compression [2–4]. Previously, this effect was demonstrated [5] but its observed saturation properties have eluded explanation [6, 7], in part because of the possibility that ion wave processes occurred in experiments with long pulse lengths [8–12], which could have masked the effect of electron kinetic saturation processes. However, since

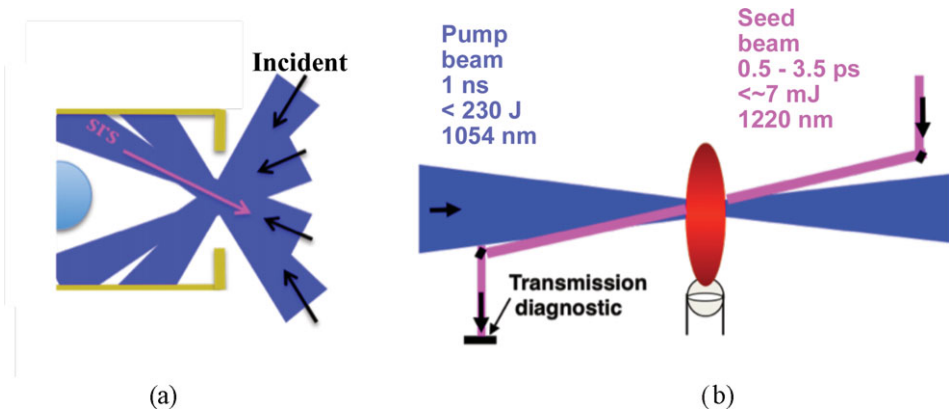


Figure 1. (Colour online) The geometry of the right half of an indirect drive ignition target is shown schematically in (a) with the Raman scattered light produced by a single beam in the interior of the hohlraum and its propagation path out across multiple entering beams, as indicated, and (b) the experimental geometry that emulates the intersection of one entering beam and the scattered Raman light on the electron kinetic time scale.

ignition targets are expected to have conditions unfavorable for ion wave growth ($k\lambda_D \geq \sim 0.5$), the electron kinetic processes are expected to be the dominant ones [6, 7] in determining the saturated scattered power. In this paper, we describe experiments that demonstrate the amplification of a seed of long wavelength light by a single crossing pump beam on an ultra-short (<3.5-ps) time scale, during which electron kinetic effects, such as wavefront bowing and particle trapping, can saturate the waves, and verify the expected scattered power predicted by 2D VPIC. The experiment used a single crossing pump beam to emulate key aspects of the conditions in indirect drive ignition targets, where the scatter produced by individual beams in the target interior is re-amplified by the many crossing beams it encounters as it exits the target, as shown schematically in Fig. 1. In particular for the ignition target described in Ref. [13], a linear analysis of the re-amplification of SRS shows that each of the 23 quads of crossing beams acting alone in a plasma with $k\lambda_D \sim 0.65$ can re-amplify the scatter produced in the interior with a gain exponent in the range of 0.1 to 0.6, depending on details of plasma and beam conditions. Thus, in the absence of wave saturation, a linear re-amplification by all beams could be the result in $10\times$ to $> \sim 100\times$ more scattered power than is predicted by conventional single beam analysis of ignition targets [14]. This work demonstrates the accuracy of a model of the re-amplification of SRS, and the nonlinear effects that can limit the overall power scattered under similar conditions. This is the first model for the Raman scattering by multiple beams, and establishes that the low gain re-amplification of broadband seeds by multiple pumps at large angles can be saturated by electron kinetic wave nonlinearities at much lower beam intensities than with SRS from single beams alone [15, 16], which is expected to allow enhanced performance in future ignition target designs.

In this paper we report the demonstration of the amplification of a 0.5 and 3.5-ps duration seed of broad spectrum light by interaction with a single crossing pump beam in a strongly damped plasma ($k\lambda_D = 0.38$), where the amplitude gain exponent is small (~ 2), and on a time scale that does not allow ion wave instabilities, and

demonstrate, for the first time such conditions, a nonlinear, electron kinetic, saturation of the amplification that is captured in 2D VPIC simulations. The shortest pulse used allows the ion waves involved in secondary decays to undergo no more than 1 radian of oscillation ($\omega\tau_{\text{pulse}} \sim 1$), so they are unable to saturate the SRS Langmuir waves as expected for ignition targets, which may also be affected by enhanced beam spray and turbulence associated with a larger number of crossing pumps.

2. Experimental design

The experiments were performed at the Jupiter laser facility with a 230-J, 1054-nm pump beam with a 1-ns pulse length, and a $< \sim 6$ mJ, @3.5 ps, seed beam incident on a gas jet target. The f/10 pump beams focal spot was 500 micron FWHM diameter, smoothed with a phase plate and was intersected by the f/25 seed beam propagating 11° away from counter-propagating, with the best focus placed ~ 12 mm after the point of intersection with the pump, so that the two beams had approximately equal spot sizes in the intersection region. The beams intersected for a distance of 3 mm along either direction of propagation. A He gas jet was used, as described in [3, 17] and produced a gas profile with a flat top region of ~ 1.5 mm. Simulations with the Hydra code [18] of the beam incident on an initially uniform gas show a uniform plasma forms across the profile of the spot, with the electron temperature reaching a peak value of 244 eV near the end of 1-ns pulse. The 2D simulations also show that the axial profile of the density is sufficiently uniform ($\delta n/n < \sim 5\%$) to keep the two beams well within the half width of the peak of the resonance with the Langmuir waves, over the $< \sim 1.5$ mm of the plateau region of the gas jet and for the duration of the 1-ns pump pulse. To achieve these conditions in the experiments the gas pressure of the jet was adjusted to maximize the observed seed amplification near 1220 nm, as is consistent with the peak electron density in the interaction volume being $1.2 \times 10^{19} \text{ cm}^{-3}$. The resonant region of the profile was confirmed with 2D interferometric images that showed the density, and hence the Langmuir wave frequency, varying by less than the half the resonance width in a region of 1 to 1.5 mm. The seed beam is created by a 1054-nm, short pulse beam passed through a Raman gas cell filled to 150 psi with N_2O to produce the 1100- to 1300-nm spectrum shown in Fig. 2, with a pulse length chosen to be either 0.5 or 3.5 ps, as measured by an auto-correlator. The data in Fig. 2 are acquired by a spectrometer coupled with an optical fiber to pick off a portion of the seed beam as it leaves the interaction region. The transmitted seed beam is also diagnosed by a 1D CCD array, filtered with a 1165-nm to 1235-nm band pass filter, imaging the 500-micron seed spot in the center of the interaction region, and providing a 1D slice of the transmitted intensity transverse to the plane of the two beams as shown in Fig. 3. The remainder of the energy is collected by a calorimeter, which was used, on seed only shots to calibrate the other instruments.

3. Experimental results

Each figure also shows data from experiments with the seed beam only (no plasma) and the pump beam only (with plasma), at the same intensities and conditions. The spectral trace from the 'seed only' experiment is increased by $10\times$ relative to the pump + seed case in Fig. 2 to clearly show that the plasma amplifier both enhances and narrows the seed spectrum relative to the 'seed only' case, which is consistent

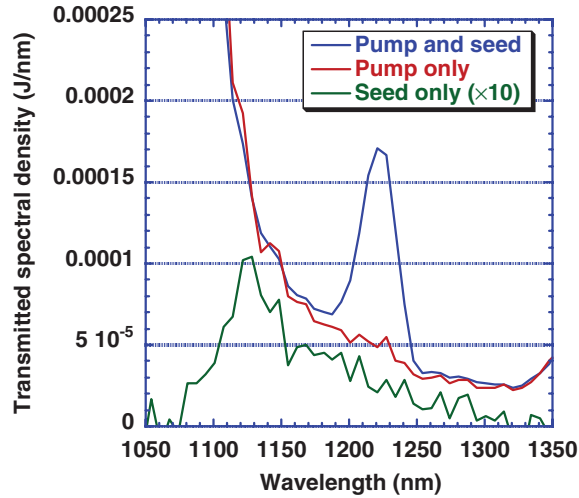


Figure 2. (Colour online) Measurement of the transmitted spectrum of the short pulse seed for the case where the pump and plasma are present, as well as a case with the seed only (shown increased 10× for clarity in this plot), indicating substantial amplification and spectral narrowing of the seed by the Langmuir wave resonance in the plasma.

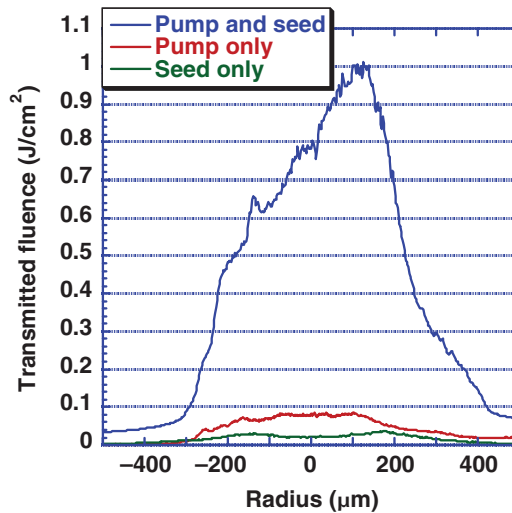


Figure 3. (Colour online) A 1D slice through an image of the 0.5-mm spot of the seed beam where it overlaps the pump beam in the plasma, for the cases of Figure 2 on the same scale, showing that the amplification occurs across the profile of the spot and is greatest near the center of the beam (43× at 60 mm) where the pump intensity is the highest, and also confirming that the amplified seed focal spot size is not significantly degraded.

with the Raman amplification in the uniform plasma region. The spectrum of un-seeded SRS from a ‘pump only’ experiment at the same pump intensity is also shown in Fig. 2, which demonstrates that the energy produced by un-seeded SRS is much less than the output seed energy and does not contribute significantly to the observed amplification. The focal spot profile data, shown in Fig. 3, also demonstrate

amplification of the seed by the pump. The observed amplification is not found to depend strongly on the timing for the seed between 200 ps and 900 ps in these experiments. The profile of the amplified seed, however, shows greater enhancement near the center of the beam, which is consistent with greater amplification where pump intensity is the highest. Further, the fact that the amplified seed profile is not broader than the spot profile of the 'seed only' case demonstrates that at the pump intensities studied in this work filamentation does not occur sufficiently to cause significant beam spray [2, 3], so the un-amplified transmitted energy is very close to the incident energy with the residual difference due mostly to plasma absorption. Inverse bremsstrahlung absorption in the plateau region of the plasma is <5% of the incident energy and does not significantly affect the amplification factor.

In order to study the response of the Langmuir waves responsible for the amplification of light on this time scale, a series of experiments were performed both with 3.5-ps and 0.5-ps seeds with the input seed power (energy) varying from 8×10^6 to 2×10^9 W. The amplification factor was calculated from the spectral and spot profile measurements as the ratio of the fluence or spectral density transmitted in the 'pump + seed' case (after subtracting that measured in the 'pump only' case as a baseline) to that transmitted in the 'seed only' case. The spectral amplification was determined at the wavelength of the peak values of the spectrally resolved energies for the three cases and found to be as high as $77\times$ for the 3.5-ps seed with an incident power of 8×10^6 W and greatly reduced or absent for incident powers ranging from 4.5×10^8 to 1.6×10^9 . The amplification factor was also measured from the spot profile data and was found to track the spectral amplification factor in the cases studied. If the waves were responding linearly to the ponderomotive force, the amplification factor would be expected to be independent of the seed power [19]. However, the data clearly show the amplification factor to be nonlinearly reduced, or saturated, at seed powers $>1 \times 10^8$ W, becoming negligible at 4.5×10^8 W, and either fluctuating or slightly increasing at the highest powers studied, as shown in Fig. 4, demonstrating the nonlinear saturation of the wave response and/or reduced coherence of the fields at high seed intensity. Moreover, we estimate the linear SRS gain rate for the simulated experimental conditions and a 1.2-mm interaction length, as shown by the line in Fig. 4, and find that the observed amplifications, especially at the highest seed intensity, are well below this value, which is also consistent with nonlinear effects reducing the wave response and scatter when the seed is large. The maximum transmitted energy in the 3.5-ps seed in these cases is $<\sim 14$ mJ, and the associated energy deposited in the plasma wave is calculated to be only <1.4 mJ. Hence, the total energy removed from the pump is $<\sim 1\%$ of the pump energy available during the 7-ps interaction period, so the saturation is not due to pump depletion. The saturation of the power scattered from the pump beam is demonstrated to be only weakly dependent on time over the 3.5-ps period, which drive the scattering Langmuir wave by a second series of measurements with 0.5-ps seed pulses. The reduced duration seed produces similar amplification factors to the longer duration case when the seed power is low, and also demonstrates a reduction of the amplification factor as the seed power is increased to 4.5×10^8 W. These measurements identify the saturation mechanism as purely electron kinetic because the saturation occurs in a time that corresponds to only one inverse wave frequency ($\tau_{\text{pulse}} \sim \omega_{\text{iaw}}^{-1}$) for the ion acoustic waves that are produced by the secondary decay of the Langmuir wave on longer time scales.

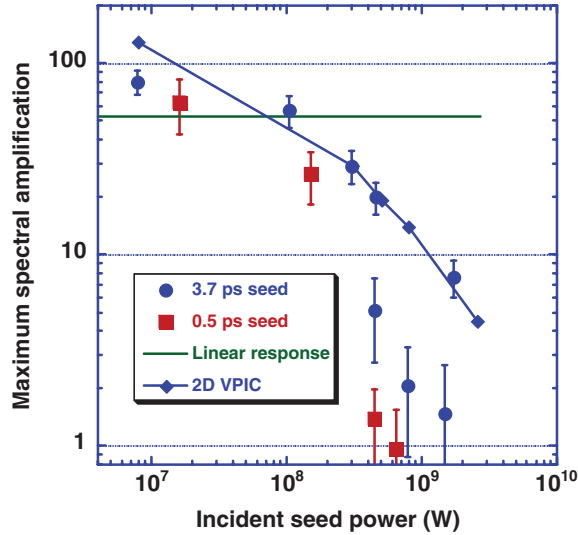


Figure 4. (Colour online) A series of experiments with varying incident seed energy are analyzed to determine the peak spectral amplification factor, and show that the amplification factor decreases significantly as the seed power is increased, demonstrating a nonlinear saturation of the scattering wave. The expected response of a linear wave and 2D VPIC simulations are as discussed in the text.

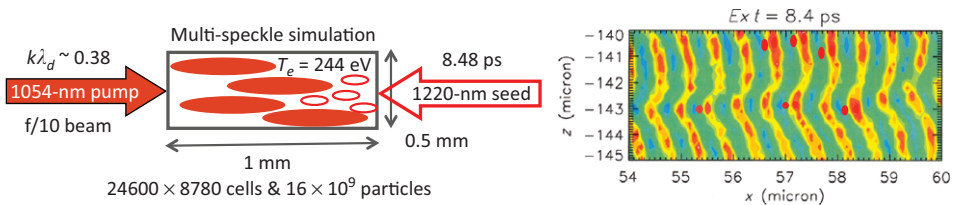


Figure 5. (Colour online) The geometry of the 2D VPIC simulations that includes a distribution of un-correlated $f/10$ speckles in the pump and seed beams with the seed 11° from counter-propagating with the pump. The simulation results show the electrostatic wave amplitude, Ex , as the seed exits the plasma, which demonstrated wave front bowing associated with the electron trapping that results in the observed nonlinear wave response.

4. Comparison with VPIC simulations

Using VPIC [20] kinetic plasma simulations with a binary collision model to treat the inter-particle Coulomb collisions [21], we have modeled the experiments in two spatial dimensions. In the simulations, the spatial domain is 1 mm in the pump laser direction and 0.5 mm in the transverse direction and the plasma is initialized with a uniform density profile having density, plasma composition, and initial temperature consistent with the experiments. The pump is a flat-top, long pulse launched from the left of the simulation domain with an average intensity of $1.02 \times 10^{14} \text{ W/cm}^2$. The seed, launched from the right of the simulation domain, is Gaussian in time with 3.5-ps full width at half maximum (FWHM) and has a central wavelength of 1200 nm; this pulse counter propagates at 11° relative to the pump direction, as shown schematically in Fig. 5. Both pump and seed intensity

profiles have random distributions of speckles of sizes equal to the diffraction-limited spot sizes; the correlation time of the speckles in the seed is set equal to twice the observed amplification spectral width to ensure that all components with significant amplification are included.

The stimulated Raman scattering initiates in the simulations when the seed and pump interact in the plasma and the amplification factor is found to decrease as the seed intensity increases, as observed experimentally. The electron distribution in the simulations also develops a supra-thermal component in the direction of the Langmuir wave, consistent with electrons being trapped by the wave. Moreover, as shown in Fig. 5, the simulations show evidence of nonlinear wave front bowing and electron plasma wave self-focusing [16], as well as an associated reduction in the amplification factor at high intensity, as seen in the experimental observations, and find that collisions significantly affect the observed amplification at low seed energy.

5. Summary

The two primary results of this paper are as follows: (1) The first observation of nonlinear saturation of scattering stimulated by a broad spectrum, short pulse seed undergoing the Raman amplification with a small amplitude gain exponent; and (2) quantitative agreement in amplification factor from experiments and first-principles, 2D PIC simulations of the electron kinetic effects. These results provide experimental benchmarks and computational tools for a model of stimulated scattering by multiple intersecting beams that can be used to optimize laser coupling in ignition experiments.

References

- [1] Lindl, J. D., Amendt, P., Berger, R. L., Glendinning, S. G., Glenzer, S. H., Haan, S. W., Kauffman, R. L., Landen, O. L. and Suter, L. J. 2004 *Phys. Plasmas* **11**, 339.
- [2] Ping, Y. et al. 2009 *Phys. Plasmas* **16**, 123113.
- [3] Kirkwood, R. K. et al. 2007 *Phys. Plasmas* **14**, 113109.
- [4] Malkin, V. M. and Fisch, N. J. 2005 *Phys. Plasmas* **12**, 044507.
- [5] Kirkwood, R. K. et al. 1999 *Phys. Rev. Lett.* **83**, 2965.
- [6] Vu, H. X., DuBois, D. F. and Bezzerrides, B. 2001 *PRL* **86**, 4306.
- [7] Sanbonmatsu, K. Y., Vu, H. X., Bezzerrides, B., Dubois, D. F. 2000 *Phys. Plasmas* **7**, 1723; Sanbonmatsu, K. Y., Vu, H. X., DuBois, D. F. and Bezzerrides, B. 1999 *Phys. Rev. Lett.* **82**, 932.
- [8] Kirkwood, R. K. et al. 1996 *Phys. Rev. Lett.* **77**, 2706.
- [9] Fernandez, J. C. et al. 1996 *Phys. Rev. Lett.* **77**, 2702.
- [10] Geddes, C. G. R., Kirkwood, R. K., Glenzer, S. H., Estabrook, K., Cohen, B. I., Young, P. E., Joshi, C. and Wharton, K. B. *Phys. Plasmas* **10**, 3422.
- [11] Montgomery, D. S., Cobble, J. A., Fernández, J. C., Focia, R. J., Johnson, R. P., Renard-LeGalloudec, N., Rose, H. A. and Russell, D. A. 2002 *Phys. Plasmas* **9**, 2311.
- [12] Kline, J. L. et al. 2006 *Phys. Plasmas* **13**, 055906.
- [13] Michel, P. et al. 2009 *Phys. Plasmas* **16**, 042702.
- [14] Hinkel, D. E. et al. 2008 *Phys. Plasmas* **15**, 056314; Divol, L. et al. 2008 *Phys. Plasmas* **15**, 056313, and references therein.
- [15] Yin, L., Albright, B. J., Bowers, K. J., Daughton, W. and Rose, H. A. *Phys. Rev. Lett.* **99**, 265004.

- [16] Yin, L., Albright, B. J., Bowers, K. J., Daughton, W. and Rose, H. A. 2008 *Phys. Plasmas* **15**, 013109.
- [17] Malka, V., Coulaud, C., Geindre, J. P., Lopez, V., Najmudin, Z., Neely, D. and Amiranoff, F. 2001 *Rev. Sci. Instrum.* **71**, 2329; Semushin, S. and Malka, V. 2001 *Rev. Sci. Instrum.* **72**, 2961.
- [18] Marinak, M. M., Kerbel, G. D., Gentile, N. A., Jones, O., Munro, D., Pollaine, S., Dittrich, T. R. and Haan, S. W. 2001 *Phys. Plasmas* **8**, 2275.
- [19] Kruer, W. L. 1988 *The Physics of Laser Plasma Interactions*. Redwood City, CA: Addison-Wesley.
- [20] Bowers et al. 2008 *Phys. Plasmas* **15**, 055702.
- [21] Takizuka, T. and Abe, H. 1977 *J. Comput. Phys.* **25**, 205.